

On the formation of neutron stars via accretion-induced collapse in binaries

A. J. Ruiter,^{1,2,3} L. Ferrario,⁴ K. Belczynski,⁵ I. R. Seitenzahl,^{1,2}
R. M. Crocker,² A. I. Karakas,⁶

¹*ARC Future Fellow, School of Physical, Environmental and Mathematical Sciences, University of New South Wales, Australian Defence Force Academy, Canberra, ACT 2600, Australia*

²*Research School of Astronomy and Astrophysics, Australian National University, Canberra, ACT 0200, Australia*

³*ARC Centre of Excellence for All-sky Astrophysics (CAASTRO)*

⁴*Mathematical Sciences Institute, Australian National University, Canberra, ACT 0200, Australia*

⁵*Nicolaus Copernicus Astronomical Center, Polish Academy of Sciences, ul. Bartycka 18, 00-716 Warsaw, Poland*

⁶*Monash Centre for Astrophysics, School of Physics and Astronomy, Monash University, VIC 3800, Australia*

February 8, 2018

ABSTRACT

Although most neutron stars are believed to form in core-collapse supernovae, some fraction of them may form in less well-known sites. We investigate evolutionary pathways leading to neutron stars formed through the collapse of oxygen-neon white dwarf (ONe WD) stars in interacting binaries. We consider are (1) non-dynamical mass transfer where an ONe WD approaches the Chandrasekhar mass via stable mass transfer leading to accretion-induced collapse (AIC) and (2) dynamical timescale merger-induced collapse (MIC) between an ONe WD and another WD. We present rates, delay times, and progenitor properties for two different treatments of common envelope evolution. We show that AIC neutron stars are formed via many different channels and the most dominant channel depends on the adopted common envelope physics. Most AIC and MIC neutron stars are born shortly after star formation, though some have delay times > 10 Gyr. The shortest delay time (25 – 50 Myr) AIC neutron stars have stripped-envelope, compact, helium-burning star donors, though many AIC neutron stars with delay times of 50 – 100 Myr form via wind-accretion from an asymptotic giant branch star. The longest delay time AIC neutron stars, which may be observed as young milli-second pulsars among globular clusters, have a red giant donor at the time of NS formation and will eventually evolve into NS + helium WD binaries. We also discuss MIC progenitors as potential gravitational wave sources for future space-based missions. The formation of neutron stars from interacting WDs in binaries is likely to be a key mechanism for the production of LIGO/Virgo gravitational wave sources (NS-NS and BH-NS mergers) in globular clusters.

Key words: binaries: close – gravitational waves – stars: evolution – stars: neutron – pulsars: general – white dwarfs

1 INTRODUCTION

It is mostly accepted that accretion from a stellar companion on to a massive carbon-oxygen (CO) white dwarf (WD) either produces a Type Ia supernova, or quiescently burns into an oxygen-neon-rich (ONe)¹ WD, as it approaches the

Chandrasekhar mass limit ($\sim 1.4 M_{\odot}$). The exact burning criteria that determine what actually occurs in Nature is still a subject of debate (Nomoto & Kondo 1991; Yoon & Langer 2005; Schwab et al. 2016). It is also not completely clear what happens to even heavier, ONe or hybrid CO-Ne WDs (Siess 2006; Karakas 2014) as they approach the Chandrasekhar mass, though the general consensus is that an ONe WD will collapse to form a neutron star (NS) (Miyaji et al. 1980). If the ONe WD is able to achieve central densities of the order of $\sim 10^{10} \text{ g cm}^{-3}$, either through stable accretion from a binary companion (Hurley et al. 2010) or

¹ We note that a non-negligible fraction of other carbon-burning products, such as Mg-24, are likely to be present in the WD. However, we adopt ‘ONe WD’ to refer to all ONe-rich WDs that also include Mg.

through mergers (Saio & Nomoto 1985), electron capture reactions on Ne-20 and Mg-24 likely cause the WD to collapse before a thermonuclear runaway is able to run its full course (see also Jones et al. 2016). Thus, in addition to NSs born from traditional iron core-collapse supernovae from massive stars, and electron-capture supernovae born from degenerate ONe cores with zero-age main sequence (ZAMS; for single stars) masses $\sim 7 - 10 M_{\odot}$, we also expect a population of NSs born from the accretion-induced collapse of heavy WD stars in interacting binaries.

NSs created via single stellar evolution are born shortly after the onset of star formation with a narrow range of delay times, due to the intrinsically massive nature of their progenitors. Having said that, there is plenty of evidence showing that core-collapse supernovae from massive stars may commonly occur in binary star systems (Smith 2014), and binary interactions indeed have the effect of pushing the delay time distribution toward larger delay times (Zapartas et al. 2017). Binary evolution effects widen the mass range where ONe WDs are expected to form and enable NSs to be born with a wider range of natal kick velocities (Podsiadlowski et al. 2004) and as we will show, delay times.

The relative fraction of NSs formed via WD accretion in binaries relative to core-collapse NSs formed from massive stars will likely be higher in environments harbouring high stellar densities (Ivanova et al. 2008). It is generally assumed that millisecond pulsars (MSPs) are old NSs that were formed in core-collapse events of massive stars and then subsequently spun up via mass accretion (but see also van den Heuvel & Bonsema 1984). This ‘recycling’ scenario was first suggested by Backus et al. (1982). However, this is in tension with the evidence that at least some pulsars found among old stellar populations (e.g. globular clusters) exhibit properties consistent with those of young NSs. This anomaly can easily be explained by NSs formed via AIC (Lyne et al. 1996; Boyles et al. 2011; Tauris et al. 2013). Hurley et al. (2010) investigated formation rates of AIC NSs using population synthesis methods (see also Ivanova & Taam 2004; Ferrario & Wickramasinghe 2007; Belczynski et al. 2010b) and found that AIC systems provide a complementary, if not more important, formation pathway to MSPs than recycling. For a discussion on various formation channels leading to MSPs, we refer the reader to Smedley et al. (2017).

Given that current and future deep synoptic sky surveys (e.g. SkyMapper, PTF, LSST) will continue to unveil an unprecedented number of stellar transients with unknown origin, it is of course worthwhile to predict the most promising observable signatures of different transient candidates; accreting, ultra-massive WDs being the main focus of this work. We distinguish between NSs formed by stable Roche-lobe overflow (RLOF) accretion (accretion-induced collapse, or AIC) and those formed in mergers (merger-induced collapse, or MIC) for the sake of predictions: the former may potentially be observed during their last mass transfer phase shortly before the WD collapses to a NS, while the latter progenitors will be difficult to detect without future, sensitive, space-based gravitational wave observatories (see section 3.3).²

From the standpoint of nucleosynthesis, demarcating the boundaries separating the conditions for WD collapse versus thermonuclear explosion is critical for delineating the progenitor parameter space between NSs formed in binaries and Type Ia supernovae (Saio & Nomoto 1985; Maoz et al. 2014). This has important consequences for chemical evolution and by extension, Galactic archaeology. Calculations by Kromer et al. (2015) have shown that lightcurves and spectra of near-Chandrasekhar mass hybrid CONe WDs that undergo a so-called ‘failed deflagration’ could explain faint Type Iax supernovae, such as 2008ha, but do not appear to be able to explain ‘normal’ Type Ia supernovae. Marquardt et al. (2015) calculated lightcurves and spectra of thermonuclear supernovae arising from exploding ONe WDs, and though there are some similarities with 1991T-like (very luminous) events, there is no clear match to a particular transient subclass, substantiating the widely-held belief that ONe WDs do not explode (see also Wu & Wang 2017). However, A recent multidimensional hydrodynamical study by Jones et al. (2016) found that collapse of an ONe WD to a NS can be avoided in cases where the assumed semi-convective mixing during the electron-capture phase preceding the deflagration is inefficient (resulting in lower central densities at ignition). In these cases the oxygen deflagration results in a weak explosion that leaves behind a bound remnant containing some iron-group material (see also Vennes et al. 2017). The higher central density cases, reflecting very efficient semi-convective mixing, on the other hand showed clear signs of collapse of the WD to a NS.

An AIC to a NS is indeed expected to be a faint event, certainly compared to ‘normal’ thermonuclear supernovae, and also compared to iron core-collapse supernovae. Electron-capture supernova explosions (see Section 2) are predicted to have much lower explosion energies ($\lesssim 10^{50}$ erg, Dessart et al. 2006; Metzger et al. 2009) compared to other core-collapse SNe whose typical explosion energies are $(0.6 - 1.2) \times 10^{51}$ erg. In the case of an AIC to a NS, ejecta masses have previously been estimated to be in the range of a few $\times 10^{-3}$ to $\sim 0.05 M_{\odot}$ (Dessart et al. 2006; Darbha et al. 2010; Fryer et al. 1999). Even though double NS mergers remain the favoured site for explaining most r-process material (Côté et al. 2017b), if the conditions for AIC are similar to those of simulated electron capture SNe, it is reasonable to suppose that AIC events could provide one of the elusive formation sites for the weak r-process (Wanajo et al. 2011; Cescutti & Chiappini 2014). By providing physical properties of the binary systems that we predict will produce NSs via induced-collapse (both stably-accreting and mergers) from binary evolution population synthesis, we hope to motivate further, detailed studies of interacting ultra-massive WDs. In addition, recent works have proposed that AIC and/or MIC NSs could potentially give rise to other exciting phenomena as well, including fast radio bursts (FRBs, Moriya 2016), magnetars (Piro & Kollmeier 2016), and gamma ray bursts (Lyutikov & Toonen 2017), and they could make an important contribution to gravitational wave astronomy (see Sec 3.3, and Lipunov 2017). More specifically: NSs that are formed by induced-collapse channels can contribute toward

² Though for MIC progenitors, the merger itself may indeed involve an electromagnetic counterpart, especially if a large amount

of mass (on the order of $0.2 M_{\odot}$) is ejected during the merger (e.g. Brooks et al. 2017).

producing double NS mergers in globular clusters (Belczynski et al. 2017).

We use the STARTRACK binary evolution population synthesis code (Belczynski et al. 2008, 2002; Ruiter et al. 2014) to determine the birthrates, ages (delay times), and evolutionary pathways of binary star systems that lead to the birth of a NS. We assume two cases for NS formation: 1) an ONe-rich WD in a binary that accretes matter from its companion until it approaches the Chandrasekhar mass limit and collapses into a NS (accretion-induced collapse, or AIC) and 2) a dynamical merger of two WDs, where at least one of them is already ONe-rich, leading to the birth of a NS via mass accretion (up to Chandrasekhar) onto the more massive WD (merger-induced collapse, or MIC, Ivanova et al. 2008). It remains to be established whether the scenarios proposed above lead in reality to a NS rather than e.g. a black hole. For example, a binary system may experience two AIC events: first a WD collapsing to a NS, then the NS collapsing to a BH (Belczynski & Taam 2004). In general, the outcome clearly depends on the final mass of the object produced via collapse and on the maximum mass that can be attained by a NS (Timmes et al. 1996). However, this limiting mass is difficult to ascertain because the initial to final mass relationship for NSs is not well constrained by observations (see Margalit & Metzger 2017, and references therein). In this paper we make the assumption that all such systems will yield NSs, even in the case where the combined mass at time of WD merger exceeds $2.5 M_{\odot}$ which is the canonical upper NS mass limit assumed in STARTRACK (see Sec 3). Since the common envelope (CE) phase is the most important source of uncertainty in the formation of WDs in binaries (De Marco 2009), we employ two different parametrizations for CE evolution to bracket the (unknown) uncertainties in the formation of these systems. The two CE treatments are described in Sec 2.

2 MODEL

We use the STARTRACK rapid binary evolution population synthesis code to evolve two populations of binary stars consisting of 250,000 systems each, starting from the ZAMS. The code has undergone many updates in recent years. Updates especially relevant for the study of intermediate-mass stars include the addition of a new treatment for CE evolution (Xu & Li 2010b; Dominik et al. 2012), an updated prescription for the treatment of helium accretion on to WDs (Ruiter et al. 2014; Kwiatkowski 2015), and the fact that we now allow a WD to gain mass from a stellar companion that is experiencing wind mass loss at a high rate (Belczynski et al. 2016).

Initial orbital parameters. Initial ZAMS star masses are drawn from a 3-component power-law initial mass function based on Kroupa et al. (1993) with $\alpha_1 = -1.3$, $\alpha_2 = -2.2$, $\alpha_3 = -2.35$. The initially more massive star ($M1$) is chosen in the mass range $0.8 - 100 M_{\odot}$ while the companion's ($M2$) mass range is $0.5 - 100 M_{\odot}$. $M1$ is drawn directly from the probability distribution function given by our chosen IMF, and $M2$ is calculated by picking a value for the mass ratio $q = 0 - 1$, e.g. $M2 = qM1$, where q is chosen with a flat probability distribution. We assume circular orbits from the ZAMS rather than the thermal distribution usually adopted

in our previous work (Ruiter et al. 2009). This guarantees a higher degree of reproducibility (for comparison purposes) with other population synthesis code data, and to first order does not have a significant effect on the results.³ For the orbital separations on the ZAMS we adopt the canonical initial distribution (flat in the logarithm), up to $10^5 R_{\odot}$, with the lower limit set by:

$$a_{\min} = f_{\min} \frac{(R_{1,0} + R_{2,0})}{(1.0 - e_0)} \quad (1)$$

where $f_{\min} = 2$ is a stellar radius multiplication factor defining the minimum orbital size, $R_{1,0}$ and $R_{2,0}$ are the ZAMS radii of stars $M1$ and $M2$, respectively, and the initial eccentricity e_0 is set equal to zero in this paper. Both populations are evolved with near-solar ($Z=0.02$) metallicity (we discuss the potential impact that metallicity could have in our study in broad terms in section 4.1).

Common envelope evolution. A CE is encountered when mass from the donor star is transferred to the accretor on a timescale that is far too short for the accretor to adjust thermally to the incoming material. As a consequence, this material heats up and swells, filling the Roche lobe. Further mass loss from the donor will form an envelope engulfing both stars. The difference between the two population models is due to the difference in how the binding energy parameter λ is estimated during CE evolution. Though significant progress has been made in quantifying the CE phase numerically over recent years (De Marco et al. 2011; Ricker & Taam 2012; Ivanova et al. 2013; Ohlmann et al. 2016), we are far from a comprehensive understanding of this critical phase of binary star evolution.

In population synthesis studies the CE phase cannot be explicitly calculated but must be somehow parametrized. A common way to do this is to equate the binding energy of the envelope of the mass-losing star with the orbital energy of the binary system. The envelope will then be expelled from the system at the expense of the binary's orbital energy (Webbink 1984), which causes the orbital size to decrease, often drastically. It is reasonable to assume that the binary's post-CE separation is determined by the energy reservoirs in the system that are available, however, we do not know how orbital energy can be transferred to the removal of the envelope; in fact it may not even be a correct assumption (Nelemans 2005). Further, it is not clear which energy reservoirs are even at our disposal (internal energy, ionization energy, enthalpy, see e.g. Ivanova & Chaichenets 2011). For this reason the CE efficiency parameter α_{ce} (Livio & Soker 1988) and the binding energy parameter λ (de Kool 1990) were introduced. These parameters contain our limited knowledge on the physics of CE evolution.

Setting the change in orbital energy equal to the binding

³ Assuming $e = 0$ for every ZAMS binary may not be the most realistic assumption particularly for binaries with large orbital periods (> 2 days, see Moe & Di Stefano 2017). For interacting binaries, where separations are already rather small, we do not expect a major impact on our final results. The impact of initial eccentricity distribution on interacting binary populations will be investigated in a future parameter study.

energy gives:

$$\alpha_{\text{CE}} \left(\frac{GM_{\text{com}} M_{\text{core}}}{a_{\text{fin}}} - \frac{GM_{\text{com}} M_{\text{core+env}}}{a_{\text{init}}} \right) = \frac{GM_{\text{core+env}} M_{\text{env}}}{\lambda R_{\text{core+env}}}, \quad (2)$$

where M_{com} is the mass of the companion star (which is not losing its envelope), M_{core} is the mass of the core of the envelope-losing star, $M_{\text{core+env}}$ and $R_{\text{core+env}}$ are the total stellar mass and radius of the envelope-losing star, and a_{fin} and a_{init} represent the final and initial orbital separations (post- and pre-CE), respectively.

For Model 1 we adopt the CE formalism employing energy balance (Webbink 1984) that historically was the favoured prescription used in binary population synthesis codes with $\alpha_{\text{ce}}\lambda = 1$. We refer to Model 1 as the “classic CE” model. Higher values of $\alpha_{\text{ce}}\lambda$ cause larger envelope ejection efficiencies which, in turn, lead to wider post-CE orbital separations. However, more plausibly, the mass-losing stars’ state of evolution will play a role in determining the binding energy of the envelope, and thusly will directly affect the value of the binding energy term. For this reason, we adopt a second CE model that takes the evolutionary stage of the donor into account, while keeping the efficiency parameter, α_{ce} , constant (=1).

For Model 2, we still use the same energy balance formula (equation 2) but use a more sophisticated approach to estimate the donor binding energy parameter λ . We denote this as the “new CE” model. To estimate the binding energy we use the revised fits of Dominik et al. (2012) based on the data from Xu & Li (2010b,a). Also, in STARTRACK we have introduced (Wiktorowicz et al. 2014) the possibility to take into account enthalpy arguments presented by Ivanova & Chaichenets (2011). These models allow for a physical estimate of donor star binding energy that depends on stellar mass, as well as its evolutionary stage and chemical composition (e.g., larger values of λ for more evolved donors). In the new CE model, the binding energy parameter value ultimately depends on the evolutionary state of the donor when the CE starts. Using Table 1 of Ivanova & Chaichenets (2011) for intermediate-mass stars as a guide, we increase the binding energy parameter (estimated from our new mass and evolutionary stage-dependent λ approach) by a factor of 2, thereby decreasing the binding energy by a factor of 2.

Stable RLOF on WDs. For binaries in RLOF (the AIC progenitors), we assume that mass accretion proceeds with the same prescription for ONe WDs as it does for CO WDs (see Ruiter et al. 2009, 2014, for hydrogen-rich and helium-rich accretion, respectively), being dependent on the rate at which mass is transferred toward the accretor, and on the mass of the accreting WD. Thus our adopted prescription is slightly different from the one adopted in Hurley et al. (2010), which assumes no mass-dependence on the WD accretor for the accretion rate. We also assume that mass transfer of CO (or ONe) on a CO or ONe WD is fully conservative (see Belczynski et al. 2008, for further details on how mass transfer phases are calculated).

Stellar winds. STARTRACK employs various prescriptions from the literature for the treatment of stellar winds. For low-mass stars, we adopt the wind prescription of Hurley et al. (2002) (see Belczynski et al. 2010a, for further details), while for Wolf-Rayet helium stars the wind prescription is based on Hamann & Koesterke (1998), with a metallicity-dependence adopted from Vink & de Koter (2005). For low-

and intermediate-mass evolved stars, it is reasonable to assume that some material lost by the donor may be accreted by a close companion. In fact, such assumptions are likely necessary for re-producing observed properties of carbon-enhanced metal-poor stars (Abate et al. 2013). We assume that a WD can accrete mass from the wind of a nearby companion AGB star donor assuming a Bondi-Hoyle accretion configuration, though this assumption may be conservative, since some simulations have shown wind accretion efficiency from evolved donor stars could be notably higher (Mohamed & Podsiadlowski 2007). For our AIC progenitors with AGB donors, the time-averaged accretion rate is $\sim 10^{-8} M_{\odot}$ per year. This AGB wind accretion model is capable of producing AIC NSs from ONe WDs that are born with masses already very close to the Chandrasekhar mass limit.

Neutron star formation. There are different ways in which a NS can form from an intermediate-mass star. Electron-capture supernovae (ECSNe) form NSs via the collapse of a degenerate ONe core (Nomoto 1987; Jones et al. 2013; Woosley & Heger 2015). The ZAMS mass of an ECSN progenitor is not extremely well-constrained since it will depend on stellar wind mass loss suffered by the star as well as binary interactions, if applicable. However, the helium core mass at the base of the AGB is thought to be $\lesssim 2.5 M_{\odot}$ (see Chruslinska et al. 2018, and references therein). ECSNe are expected to comprise roughly 4 per cent of all core-collapse supernovae (Wanajo et al. 2011).

The main difference between the progenitors of ECSNe and AIC is that the ONe core of an ECSN precursor is still surrounded by He- and H-burning shells, which allows the ONe core to grow in mass, collapse, and subsequently suffer a deflagration (Hillebrandt et al. 1984). This different configuration may affect the resulting nucleosynthesis during and possibly also after the formation of the NS. In this work we do not discuss general ECSN formation channels but focus on the sub-population of NSs formed through evolutionary channels that involve the collapse of a WD star in an interacting binary. Below, we summarise the conditions for AIC and MIC.

Today, one of the most promising progenitor scenarios for the formation of Type Ia supernovae is the merger of two CO-rich WDs (Nomoto & Iben 1985; Pakmor et al. 2010, 2012; Ruiter et al. 2013; Tanikawa et al. 2015), with some support for CO WDs merging with He-rich WDs (Dan et al. 2015; Fenn et al. 2016; Crocker et al. 2017; Brown et al. 2017). It is still under investigation whether the WD merger proceeds via ‘accretion up to Chandrasekhar’, in which case the explosion mechanism would likely be similar to the classic single degenerate scenario (e.g. Röpke et al. 2007; Seitenzahl et al. 2013), or occur via prompt detonation such as the ‘helium-ignited violent merger model’ of Pakmor et al. (2013) (see also Shen & Moore 2014). Analogous to CO WDs, in our binary evolution population synthesis simulations concerning ONe WDs we do not differentiate between the two types of merger scenarios, and we include all heavy WD mergers as potential MIC candidates. For the MIC scenario, we assume that a NS is formed any time an ONe-rich WD merges with another WD regardless of its composition or total mass (which always exceeds $1.5 M_{\odot}$, see Sec. 3). In our models, ONe WDs only merge with CO WDs or ONe WDs. This is because for other, less-massive WD types (e.g. He-rich), the mass ratio is far from unity and thus when the

less-massive WD fills its Roche-lobe mass transfer is dynamically stable, and a merger is avoided in our models (cf. Côté et al. 2017a, section 6.2). For instance, most of the observed AMCVn systems, which are short period binaries where a He-rich star (thought to be a white dwarf) transfers mass to its more massive WD companion exhibit dynamically stable mass transfer, although it has been suggested that some of these binaries, whose mass ratios are closer to unity, may undergo explosive events such as SNe Ia or SN Ia (Bildsten et al. 2007; Perets et al. 2010).

In the AIC scenario, we assume that when any ONe WD approaches the Chandrasekhar mass limit via stable accretion, a NS is formed. Although STARTRACK can follow the evolution of each system after the formation of the NS, this is beyond the scope of the present work to examine the future evolution of the entire AIC population. However, we comment briefly on the future evolution of some AIC binaries in section 4.

3 RESULTS

3.1 Progenitors and delay times

We find that AIC and MIC systems occur with a full range of delay times. Though both AIC and MIC NSs can be born up to a Hubble time (or beyond) after star formation, most are formed within 200 Myr after starburst.

3.1.1 AIC donor types

In Fig 1 and Fig 2 we show number density plots of donor star companion type vs. delay time for the binary systems that undergo AIC for our classical and new CE models, respectively. The numbers are raw data and thus not calibrated to fit the characteristics (e.g. star formation rate over time) of the Milky Way. Though the overall AIC birthrates are similar for both CE models (see section 3.2), there are some notable differences between them, that is, 1) there are no AIC systems with WD donors in the new CE model at the time when AIC occurs, though such progenitors are common in the classical CE model; 2) in the new CE model, AIC progenitors with AGB donors dominate strongly over all other binary types, while H-envelope-stripped, helium-burning stars and hydrogen-rich giant-like stars contribute to the distribution quite strongly in the classical model.

In both CE models, the shortest-delay time AIC systems are those with H-envelope-stripped, helium-burning (mostly with a defined core-envelope structure, e.g. helium subgiants) or AGB donors (< 50 Myr after starburst). The shortest delay time NS in our models is found in the New CE model, at a delay time of 31 Myr with a stripped-envelope, compact helium-burning star donor (sometimes referred to as a main sequence helium star). The initial masses of the stars were 10.7 and 9.1 M_{\odot} with an initial separation of 977 R_{\odot} . The longest delay time systems, e.g. those that plausibly represent the population of ‘young’ NSs found among globular clusters, mostly have giant-like donors that have maintained their H-rich envelopes, though a minority of systems have MS donors (the latter are found in the classical CE model only). We describe some specific evolutionary channels in the Appendix.

3.1.2 MIC white dwarf masses

In Fig 3 and Fig 4 we show number density distributions of the total WD mass at time of merger as a function of delay time for the classical and new CE models, respectively. Some massive binaries merge at late delay times for both CE models. These systems go through one CE event, rather than two CE events; the latter are common for the events with delay times < 1 Gyr. Note that in some systems it is the same star that undergoes a CE twice (first losing its hydrogen envelope, then later its helium envelope, see Ruiter et al. (2013)). Just like AIC NSs, MIC NSs can form at very long delay times.

We overplot with a dashed line the maximum NS mass that is normally allowed in STARTRACK (2.5 M_{\odot} is the typically-chosen parameter value). There are not many events above this threshold in either model, though we assume that in the event that a NS is born, any mass above this threshold would have to leave the system to avoid collapsing to a black hole. We also show with a dot-dash line the upper mass limit expected for a NS from the recent study of Margalit & Metzger (2017), who find a maximum NS mass of only 2.17 M_{\odot} . We find ~ 50 per cent and ~ 20 per cent of our MIC systems lie above 2.17 M_{\odot} in our classical and new CE model, respectively. However, in the new CE model, about 90 % of these massive systems form through an evolutionary channel that involves a CE phase while the mass-losing star is only a slightly-evolved giant, and other works have pointed out that such systems are less likely to undergo a CE phase (see Discussion). On the other hand, in our classical CE model, a smaller fraction (~ 60 %) of the NS progenitors $> 2.17 M_{\odot}$ encounter a CE during the same (Hertzsprung Gap) evolutionary phase. This means that 40% (vs. 10%) of the systems above 2.17 M_{\odot} have a likely chance of survival of this CE phase and subsequent evolution toward MIC. Thus, if our models are any indication of how CE physics behaves in Nature, future detections of stellar mass black holes $> 2.17 M_{\odot}$, if formed via binary evolution, would indicate that CE physics behaves more closely to what we have assumed for the classical CE model.

In Fig 5 and Fig 6 we show number density distributions of primary vs. secondary WD mass (initially more massive vs. initially less massive star). For comparison, a similar figure in Lyutikov & Toonen (2017) (see their figure 5) has a sharp discontinuity along the primary mass range $\sim 1 - 1.1 M_{\odot}$, though we note that they only consider CO+ONe WD pairs in their models (no double ONe WD pairs). It is not surprising that the different population synthesis codes reproduce similar results in terms of predicted pre-merger WD masses (see also Toonen et al. 2014). The different regions of ‘clumps’ is a result of different evolutionary channels (see sect. 3.3).

3.2 Birthrates

We predict birthrates of AIC and MIC systems for our binary star populations. Our rates are calibrated per unit mass formed in stars and are calculated by assuming a binary star fraction of 70 per cent. We find a current Galactic birthrate of $\sim 3 \times 10^{-4} (\pm 2 \times 10^{-4})$ events per year, for both MIC and AIC (e.g. a total induced collapse rate of $\sim 6 \times 10^{-4}$ events per year), assuming a constant star formation rate

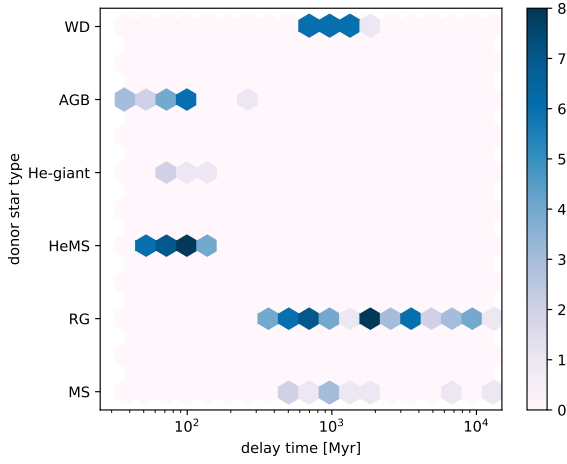


Figure 1. Number density distributions of delay time vs. donor star type at time of AIC for the classical CE prescription. The darker the colour, the higher the concentration of systems in the parameter space (see colourbar).

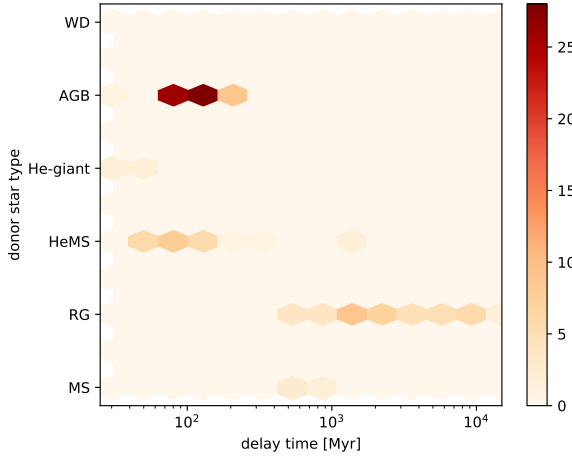


Figure 2. Like Figure 1: Number density distributions of delay time vs. donor star type at time of AIC for the new CE prescription.

(see below). We find no significant change in birthrate with adopted CE model, though we note the rate of MIC mergers is slightly lower for the new CE model, owing to the lower number of close ONe+ONe WD systems produced. In our classical CE model, 15 per cent of MIC systems consist of ONe+ONe WD pairs, and the rest are CO+ONe WD pairs. In the new CE model, only 3 per cent are ONe+ONe WD pairs because many double ONe WD systems never end up on close enough orbits to merge within a Hubble time. The explanation for the lower number of ONe+ONe mergers in the new CE model is as follows. The main difference between the progenitors of ONe+ONe mergers and those of ONe+CO mergers is that ONe+ONe mergers typically undergo only one CE phase whereas CO+ONe mergers normally undergo two CE phases. For the ONe+ONe MIC progenitors, the single CE event happens when the donor star is only slightly

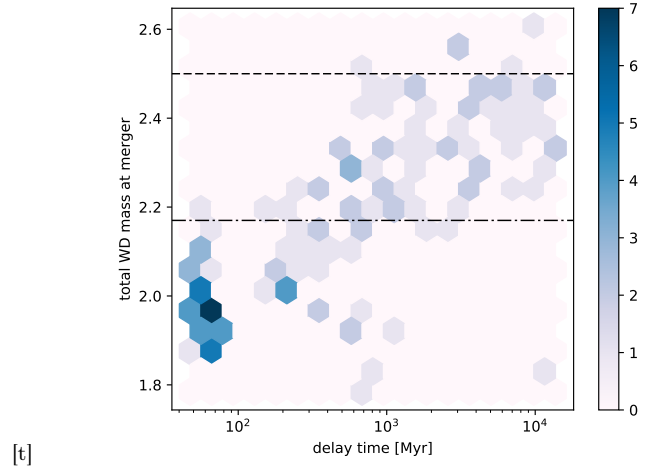


Figure 3. Number density distributions of delay time vs. total WD mass at time of MIC for the classical CE prescription. Horizontal lines correspond to the assumed neutron star upper mass limit, above which the compact object is likely to become a black hole in STARTRACK (dashed line) and [Margalit & Metzger \(2017\)](#) (dot-dashed line, see text).

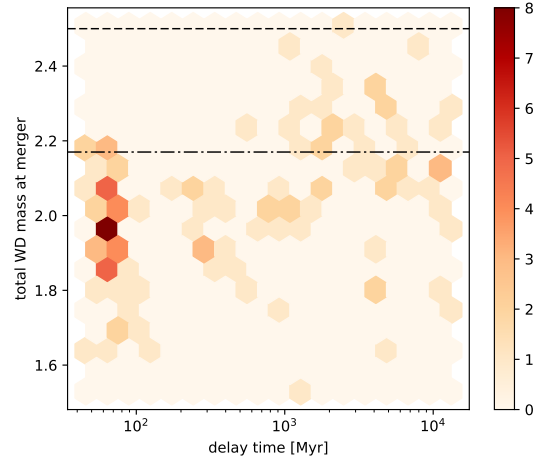


Figure 4. Number density distributions of delay time vs. total WD mass at time of MIC for the new CE prescription. Horizontal lines correspond to the assumed NS upper mass limit, above which the compact object is likely to become a black hole in STARTRACK (dashed line) and [Margalit & Metzger \(2017\)](#) (dot-dashed line, see text).

evolved (a red giant or in the Hertzsprung gap), so that it would still have a higher binding energy parameter λ in the new CE model (by a factor of a few) compared to the classical CE model ($\lambda = 1$; see section 2). As a consequence, the binding energy of the donor star in the new CE model is lower so the separation of the stars after CE is somewhat wider, and the binary never achieves contact again within a Hubble time. We comment on the likeliness of binary system survival during a CE phase when the giant-like donor does not have a strongly distinct core-envelope structure in section 4.

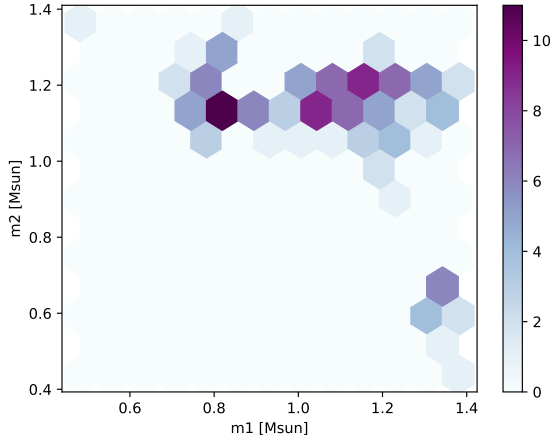


Figure 5. Number density distributions of WD masses at time of merger for the initially more massive star (x-axis) and initially less massive star (y-axis) for the classical CE prescription.

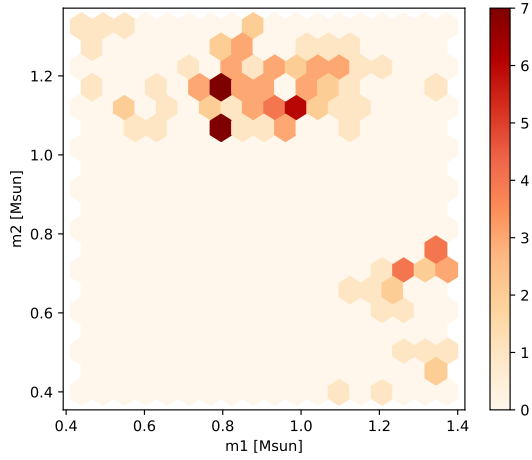


Figure 6. Number density distributions for WD masses at time of merger for the initially more massive star (x-axis) and initially less massive star (y-axis) for the new CE prescription.

CE model	Type II	Type Ib, Ic	AIC	MIC	SN Ia (DD – CO only)	SN Ia (SD)	SN Ia (ddet)	SN Ia (DD – faint)
Classical	12177	6725	123	136	3208	53	4335	239
New	12207	5484	139	122	1383	60	2775	1206

Table 1. Relative total number of events from STARTRACK that occur per simulation of 250,000 ZAMS binaries that are allowed to evolve for 13.7 Gyr. We show relative rates of core-collapse supernovae, neutron stars formed via induced-collapse (AIC and MIC), and 4 scenarios of thermonuclear supernovae. SN Ia (DD – CO only): All mergers between two CO WDs. SN Ia (SD): All CO WDs that reach the Chandrasekhar mass via accretion from any companion. SN Ia (ddet): All sub-Chandrasekhar mass CO WDs that achieve double detonation via (slow) He-accretion. SN Ia (DD – faint): Mergers between a CO WD and a pure helium WD (see text).

For birthrates we have assumed the same simple star formation history of $6 \text{ M}_\odot \text{ yr}^{-1}$ that was adopted in [Lyutikov & Toonen \(2017\)](#). Our MIC birthrates are nearly identical to those of [Lyutikov & Toonen \(2017\)](#): $\sim 2 - 5 \times 10^{-4} \text{ M}_\odot \text{ yr}^{-1}$, depending on their adopted CE formalism. Our predicted Galactic AIC rates are somewhat higher than those forecast by [Yungelson & Livio \(1998\)](#) that amount to 8×10^{-7} to 8×10^{-5} events per year. When comparing our AIC birthrates to the binary millisecond pulsars formed via AIC of [Hurley et al. \(2010\)](#)⁴, our numbers are within agreement (see their table 1) if we make the assumption that all AICs make MSPs. This is justified considering that conservation of angular momentum would naturally cause the NS to spin at millisecond periods and the conservation of magnetic flux would produce a NS with magnetic fields in the range $10^8 - 10^9 \text{ G}$, typical of MSPs, without having to invoke accretion induced field decay ([Ferrario & Wickramasinghe 2007](#); [Smedley et al. 2015](#)). On the other hand, [Tauris et al. \(2013\)](#) pointed out that the formation of NSs may be inevitably accompanied by the generation of strong magnetic fields, and thus these AIC NSs would need to undergo further accretion to reach the observed weaker fields.

We note that our predicted Galactic rates of AIC events are in agreement with upper limit estimates set by solar system abundances of neutron-rich isotopes, which is $\sim 10^{-4}$ AIC per year ([Fryer et al. 1999](#); [Dessart et al. 2006](#); [Metzger et al. 2009](#)). Though it remains to be confirmed which isotopes are synthesized in AIC events, if AIC NSs are indeed a formation site for a sub-set of neutron-rich isotopes (including r-process), local abundance patterns could potentially provide a useful lower limit on Galactic AIC formation rates ([De Silva et al. 2015](#)). If we consider the fact that AIC NSs may leave behind a hot remnant of ionised gas that is potentially visible for up to 100,000 years, analogous to what has been predicted for the Chandrasekhar mass (i.e. single degenerate) scenario of Type Ia supernovae ([Woods et al. 2017](#)), we estimate that on the order of 10 of these post-AIC remnants could currently exist in the Galaxy today.

In Table 1 we show relative formation rates (over a Hubble time) for neutron stars formed through different channels (including core-collapse supernovae), as well as thermonuclear supernovae. For core-collapse of massive stars, we include full SN explosions, fall-back (low-energy) explosions and direct collapse to black hole ([Fryer et al. 2012](#)). For thermonuclear supernovae, we include four potential formation scenarios (see table caption), including the possible progenitors of 1991bg-like supernovae which could originate from mergers between CO and pure helium WDs ([Crocker et al. 2017](#)).

3.3 MIC progenitors as gravitational wave sources

It has been shown that the gravitational wave signature of Galactic double WD binaries with orbital periods of less than about 5 hours will be detectable with future space-based gravitational wave observatories, like the [evolved]

⁴ [Hurley et al. \(2010\)](#) also assumed a constant star formation history but at a higher rate of $8.6 \text{ M}_\odot \text{ yr}^{-1}$, and used different assumptions for CE evolution.

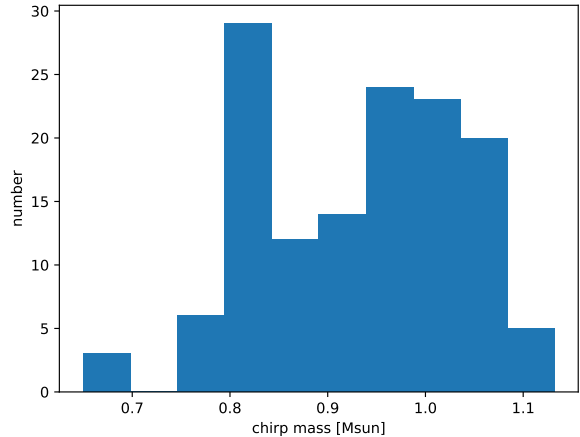


Figure 7. Chirp mass of white dwarf pairs leading to MIC events at time of merger for the classical CE model.

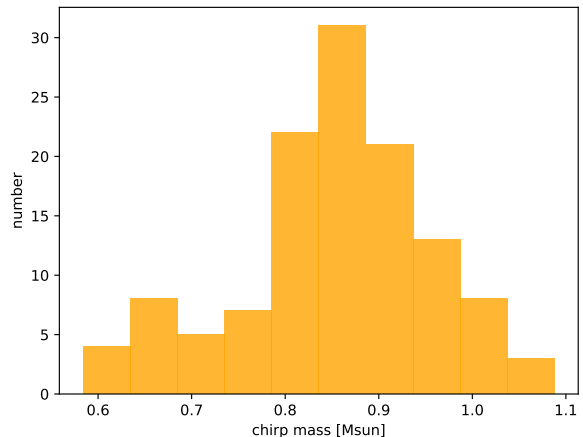


Figure 8. Chirp mass distribution of heavy white dwarf pairs at time of merger for the new CE model.

Laser Interferometer Space Antenna, [e]LISA ([Nelemans et al. 2004](#); [Ruiter et al. 2010](#); [Cornish & Robson 2017](#)). The most massive, very nearby binaries with the shortest orbital periods will have the best chance to be individually resolved as gravitational wave sources ([Nelemans 2013](#)).

A quantity that is a function of the component masses, the chirp mass $M_{\text{chirp}} = (m_1 m_2)^{3/5} / (m_1 + m_2)^{1/5}$, can be directly measured from gravitational wave signals. The (dimensionless) strain amplitude, h , is proportional to $M_{\text{chirp}}^{5/3}$, via

$$h = 2(4\pi)^{1/3} \frac{G^{5/3}}{c^4} f_{\text{GW}}^{2/3} M_{\text{chirp}}^{5/3} \frac{1}{r} \quad (3)$$

where the gravitational wave frequency of a binary with a circular orbit is $f_{\text{GW}} = 2/(P_{\text{orb}})$ where P_{orb} is the orbital period, and r is the distance to the binary from the detector. h is a measure of the fractional change in separation that occurs (e.g. between detector nodes, or spacecrafts) when a gravitational wave passes through the detector. Naturally,

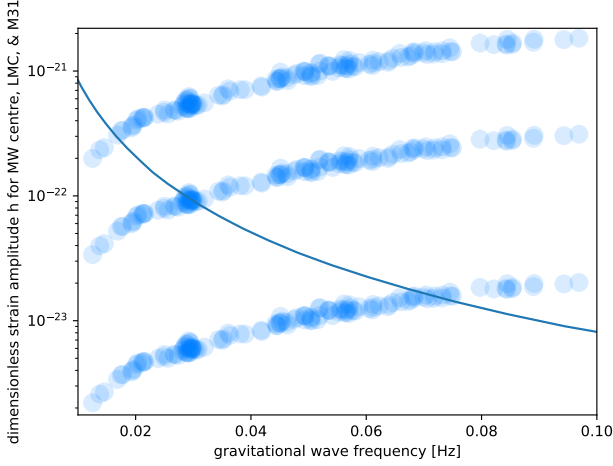


Figure 9. Gravitational wave strain amplitude of MIC progenitors at a distance of the Galactic centre (top), the LMC, and M31 (bottom) vs. gravitational wave frequency for the classical CE model at time just before merger. All binaries have circular orbits. We over-plot the sensitivity curve for the proposed future space-based gravitational wave observatory BBO from Yagi & Seto (2017).

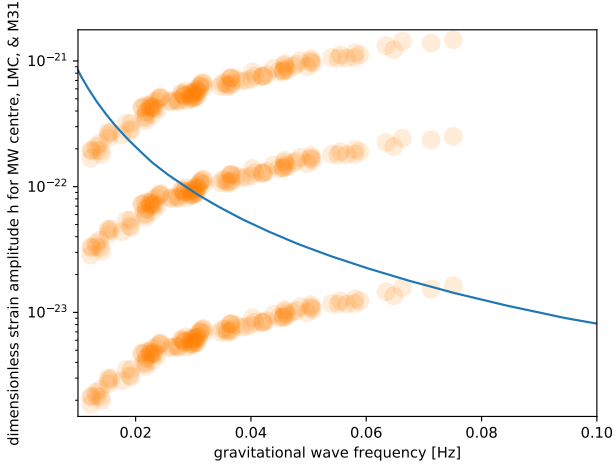


Figure 10. Gravitational wave strain amplitude of MIC progenitors at a distance of the Galactic centre (top), the LMC, and M31 (bottom) vs. gravitational wave frequency for the new CE model at time just before merger. All binaries have circular orbits. We over-plot the sensitivity curve for the proposed future space-based gravitational wave observatory BBO from Yagi & Seto (2017).

as the binary approaches merger time, its orbital period decreases drastically and thus f_{GW} increases (sweeping, or ‘chirping’ across the frequency band). Note that the orbital frequency evolution can also be negative, such as in the case of some mass-transferring binaries (Kremer et al. 2017).

In Fig 7 and Fig 8 we show the distribution of MIC progenitor chirp masses (at time of WD-WD merger) for the classical and new CE approaches, respectively. Correspondingly, in Fig 9 and Fig 10 we show the gravitational wave amplitude for both models, assuming distances of 8.5 kpc from the Galactic centre, 50 kpc from the LMC and 770 kpc

from M31. The distribution of chirp masses is bimodal in the classical CE model, but it has only one peak in the new CE model. This effect is reflected in the strain vs. gravitational wave frequency plots (see below). The reason for the different distribution shapes is attributed to the different formation channels that dominate depending on the CE model. The fact that different formation channels are more (less) prominent than others depending on the CE model results in a different ranges of chirp mass being more (less) populated than others.

In the classical CE model, two main peaks are visible in Fig 7: the highest peak is $\sim 0.82 M_{\odot}$, and another broader peak centered $\sim 1 M_{\odot}$ (see Example 2 in the Appendix). The first peak corresponds to progenitors with delay times less than 300 Myr arising from different formation channels. The systems with chirp masses below $\sim 0.79 M_{\odot}$ are almost exclusively arising from progenitors with delay times greater than 300 Myr that undergo two CE events: first when the primary is an AGB star, then later when the secondary is a red giant. These MIC systems populate the lower-right quadrant of Fig. 5.

In the new CE model for MIC progenitors, the peak in Fig 8 $\sim 0.86 M_{\odot}$ is dominated by two formation channels: one short (~ 70 Myr) delay time channel (see Appendix example 3) and one long (~ 11 Gyr) channel. The systems that populate the parameter space with lower chirp masses consist mostly of short delay time MIC binaries that undergo one stable mass transfer event (primary star loses mass to secondary), and two CE events (primary and then secondary star losing envelope, or secondary star loses its envelope: first hydrogen envelope then later the helium envelope). These MIC systems populate the lower-right quadrant of Fig. 6. The binaries populating the higher chirp mass part of the distribution are almost exclusively from one formation channel with very short (~ 40 Myr) delay times and the following mass transfer phases: 1. stable mass transfer from a Hertzsprung Gap star (primary) toward main sequence star, 2. stable mass transfer from a naked helium-giant (primary) to a main sequence star, 3. a CE phase between a (secondary) star in the Hertzsprung Gap and a CO WD, and 4. stable mass transfer between a H-envelope-stripped helium-burning giant (secondary) and the CO WD. This final phase is the higher mass analogue of what occurs during the evolution of some Type Ia supernova progenitors (stage VIII) uncovered in Ruiter et al. (2013).

If binaries in fact do survive a CE phase that involves a Hertzsprung Gap star (see section 4), then our predictions indicate they will have some of the highest chirp masses among the double WD binary population. We look forward to the time when gravitational wave measurements of close binary stars could be able to finally confirm or refute such predictions of CE evolution.

Future first-generation space-based gravitational wave observatories like LISA should be able to detect nearby MIC progenitors within our own Milky Way, but will face difficulty in resolving large populations of these relatively rare systems. Characterising the physical properties of induced-collapse progenitors could be more easily realised with the aid of more sensitive instruments, such as DECIGO and BBO (Big Bang Observatory; see Yagi and Seto 2017). BBO and DECIGO will have higher sensitivity and their bandwidths will go to higher gravitational frequencies, which cor-

respond to the (shortest) orbital periods that the MIC progenitors will have shortly before they merge. Over-plotted in Fig 9 and Fig 10 is the expected sensitivity curve for the future space-based gravitational wave observatory Big Bang Observatory. Figs 9 and 10 show that BBO will be sensitive to MIC progenitors external to the Milky Way. This exciting fact may allow for sufficient statistical information to be collected for these sources to enable the community to set constraints on phases of close binary star interactions, namely CE evolution. This will have important consequences not only for MIC NSs, but also SN Ia progenitors. As currently planned, BBO should be able to detect double WDs that will impose a strain amplitude as high as $\sim a \text{ few } \times 10^{-22}$ at 0.02 Hz (100 s orbital period).

We remind the reader that we have plotted the gravitational radiation frequencies that correspond to the MIC progenitors just before the WDs merge. If we take the binary evolution backwards in time, the number density distributions travel in the negative x-direction, and the most nearby (Galactic) systems would be readily detected (if not resolved) in the LISA band (see Moore et al. 2013).

As expected, our results indicate that nearby (Galactic) binaries will have the best chance of being detected (i.e., the upper distribution of points in both figures lies mostly above the BBO sensitivity curve). It will be extremely difficult to detect MIC progenitors as far out as M31, except for the shortest-orbital period systems, which are only predicted in our classical model (Fig. 9). The classical CE model produces a larger number of double WD binaries where both components have a high mass compared to the new CE model.⁵ The massive binaries are more compact thus are able to attain smaller orbital periods before being driven toward dynamically-unstable mass-transfer (and merger) due to orbital angular momentum losses suffered via gravitational radiation emission. It is certainly worth noting that, regardless of how the CE phase behaves in Nature, MIC progenitors should be detectable in gravitational waves, in fact they could even be resolved, both in the Galaxy and in the Magellanic clouds. Though their birthrates will likely be lower in the Magellanic Clouds than in the MW owing to the smaller stellar mass of the LMC and SMC, the fact that the LMC and SMC are more actively star-forming (per unit stellar mass) means that the MIC birthrates may not be too far off from those we predict for the MW.

4 DISCUSSION

We note that we did not find any induced-collapse systems where a CO WD is produced first, then evolves into an ONe WD via accretion and subsequent carbon shell flashes. This scenario was recently discussed in Brooks et al. (2017), and those authors state that this may be a significant formation channel leading to AIC events. In our simulations, all AIC progenitors of ONe WDs have masses above $7 M_{\odot}$ on the ZAMS and, at the base of the AGB, their cores are above the minimum value (threshold between forming CO

core and ONe core) that is needed to form an ONe WD (in STARTRACK). Our models predict some AIC systems that are similar to those considered in Brooks et al. (2017) (a H-envelope-stripped helium-burning star donor with a mass $\sim 1.5 M_{\odot}$ when the final, pre-AIC mass transfer starts). The following example is found in our new CE model: The AIC progenitor’s evolutionary channel consists of several mass exchange events (including two CE events) with an AIC occurring about 150 Myr after star formation. The NS+He star binary survives to later briefly re-establish stable mass transfer between the H-envelope-stripped helium-burning star and the NS. By a Hubble time, the system has evolved into a NS+COWD binary with component masses 1.26 and $0.74 M_{\odot}$, respectively, with an orbital period of ~ 0.5 days. Such systems could be the higher mass analogues of systems that appear as “redbacks”. Redbacks are binary MSPs with orbital periods shorter than about 1.5 d, low to zero eccentricities, and the pulsars’ companions have minimum masses estimated to be in the range $\sim 0.1 - 0.5 M_{\odot}$ (Smedley et al. 2015; Manchester et al. 2005). These systems exhibit long radio eclipses caused by circumbinary discs and do not lie on the $M_c - P_{orb}$ relation for MSPs with He WD companions. Smedley et al. (2015) proposed that redbacks and some black widow pulsars could be the result of the AIC of an ONe WD. In STARTRACK, we find that those AIC systems that end up with low-mass WD companions (e.g. at a Hubble time) and evolve to closely resemble redbacks, tend to undergo AIC when the donor is a red giant star. Thus these AICs would have much longer delay times than those systems described in Brooks et al. (2017) (see Figs. 1 and 2). Further, these STARTRACK redback systems undergo a long-lived (> 10 Myr) phase of mass transfer from the red giant to the NS, which is probably needed to spin up the NS. After RLOF ceases, the red giant eventually evolves into a low-mass helium star. Our current study clearly supports the AIC route for the formation of this exotic class of MSPs.

Despite the fact that there are no NS+WD binaries at time of collapse in the new CE model, for both CE models nearly all AIC systems do eventually (e.g. within a Hubble time) evolve into NS+WD binaries. We note that for over 90 per cent of AIC systems from our models, the companion star has evolved into a WD by a Hubble time. In cases where the companion is not a WD by a Hubble time it is almost always a H-envelope-stripped, helium-burning star (e.g. a CO WD progenitor). Observations (see Manchester et al. 2005) show that nearly 50 per cent of binary MSPs (about 60 per cent of the total population) have a helium-WD companion, 10 per cent a COWD, 10 per cent are redbacks and about 20 per cent have an ultralight companion (a substellar object or planet). Thus our synthetic AIC population is in general agreement with current observations of MSPs, while the NSs forming via MIC will contribute to the population of isolated MSPs. We also note the formation of a few widely separated (though still bound) double NS binaries (separations of about $10^4 R_{\odot}$). In this case both ZAMS masses were in the narrow range $7.5 - 7.8 M_{\odot}$.

As mentioned previously, some formation channels require the CE phases to occur while the mass-losing star is only a slightly evolved giant, e.g. in the Hertzsprung Gap. However, the assumption that a binary can survive such a CE phase is rather optimistic. Stars in the Hertzsprung Gap have a more poorly-defined core-envelope structure as com-

⁵ If we simulate binary examples from the ZAMS with the same initial orbital configuration but employ the new CE model set-up, the binaries generally do evolve into double WDs, but they do not merge within a Hubble time.

pared to more evolved red giants or AGB stars that have a well-defined jump in specific entropy between the core and envelope (Belczynski et al. 2007). Further, stars that we have found to undergo significant mass loss (and initiate a CE phase) while in the Hertzsprung Gap may rather experience stable mass transfer instead (Pavlovskii & Ivanova 2015), which would change the evolutionary outcome of the binary altogether, likely lowering the number of potential MIC systems arising from certain formation channels.

4.1 Globular clusters and the influence of initial helium fraction

We find that induced-collapse NSs can be born at any delay time ranging from ~ 30 Myr to a Hubble time and beyond (see section 3.1). It has long been postulated that a low kick velocity channel for the production of NSs may be required to explain the large excess of these objects in globular clusters (Katz 1975). Core-collapse supernovae may result in large natal kick velocities being imparted upon their newly-formed NSs, owing to asymmetries that arise in mass ejection and/or neutrino emission (Janka 2017; Fryer & Kusenko 2006). MSPs derived from AIC are expected to suffer much smaller natal kicks than delivered to NSs resulting from core-collapse supernovae (e.g. Freire & Tauris 2014, and references therein). This may help to explain how, despite their shallow gravitational wells, so many MSPs can be present in globular clusters (Grindlay 1987; Bailyn & Grindlay 1990; Benacquista et al. 2001; Podsiadlowski et al. 2004; Ivanova et al. 2008; Freire 2013).

It is a worthwhile exercise to consider how different chemical environments can influence the formation of compact objects. In particular, enhancement of helium on the ZAMS can have a significant effect on the final evolution of the star – whether it evolves into a CO WD, ONe WD, or NS (Shingles et al. 2015). HST photometry has revealed that some metal-poor Galactic globular clusters host extremely helium-enhanced stellar populations, with helium abundances up to $Y \approx 0.4$ (Gratton et al. 2012). However, globular clusters are not the only systems with claims of extremely helium-enhanced sub-populations. An increase in helium for the Galactic bulge has also been suggested based on observations of the red giant branch bump (Nataf et al. 2011; Bensby et al. 2013) and the discrepancy between its photometric and spectroscopic turnoff ages (Nataf & Gould 2012). Helium-enhanced sub-populations have also been suggested for early-type and spiral galaxies (Atlee et al. 2009; Chung et al. 2011; Rosenfield et al. 2012; Buell 2013).

While the effect of helium-enrichment on stellar evolution is relatively well known e.g., the main sequence luminosity will be higher owing to an increase in the mean molecular weight, most studies have focused on low-mass stars and the effect of helium enrichment on colour-magnitude diagrams (e.g., Sweigart 1987; Salaris & Cassisi 2005; Chantreau et al. 2015). Single star models of intermediate-mass that are evolved past the main sequence also show interesting behaviour, with helium-enhanced models entering the AGB with a more massive H-exhausted core compared to their primordial helium counterparts (e.g., Karakas et al. 2014). The main consequence for this study is that the minimum mass for carbon burning is reduced from $> 6M_{\odot}$ for $Y = 0.24$ to

$4 - 5M_{\odot}$ for $Y = 0.35 - 0.40$ for $[\text{Fe}/\text{H}] \approx -1.4$ (Shingles et al. 2015).

In our simulations we have adopted a canonical value for helium of $Y = 0.28$, similar to Karakas (2014). Interestingly, very metal-rich models of $Z = 0.1$ also show a decrease in the minimum mass for carbon burning to $\approx 7M_{\odot}$ compared to solar metallicity, a result which will be applicable to very metal-rich stellar populations including those found in massive early-type galaxies.

Because the stellar initial mass function (Kroupa et al. 1993) favours the production of lower mass stars, the fact that the carbon-burning mass threshold can be decreased by up to two solar masses would have noticeable consequences. Larger initial helium abundances yield a larger number of ONe WDs and correspondingly, fewer CO WDs. Thus the rate of SNe Ia from merging CO WD pairs would be decreased, as would the rate of SNe Ia involving stable accretion on to a CO WD. At the same time, we would expect the rate of ONe production, and thus the AIC and MIC rates, to increase from the predicted Galactic rate of several $\times 10^{-4}$ per year. This proposed effect might be somewhat curtailed if CO WD mergers on the lower mass end, e.g. even those WD pairs with combined masses below the Chandrasekhar mass limit, are an important contributor to SNe Ia (van Kerkwijk et al. 2010). However, even though including the lower-mass WD systems as potential SNIa progenitors brings the theoretical rate predictions into agreement with observations (Badenes & Maoz 2012; Maoz et al. 2018), the idea is still somewhat speculative since it remains to be demonstrated how the explosion would be triggered, and what the burning products might be.

5 SUMMARY

We have predicted birthrates, delay times, and the types of binary stars that make NSs produced in binary star systems containing at least one massive WD. Particularly interesting results of our study are 1) merger-induced collapse progenitor populations may be observed with sensitive space-based gravitational wave detectors, which could give us information about CE physics 2) induced-collapse NSs can be born at extremely early times after the onset of star formation, e.g. 30 Myr, as well as at extremely late times (Hubble time), and 3) in the AIC scenario, different types of donor stars are responsible for pushing the accreting WD over the Chandrasekhar mass, and except for the AGB-wind donor case, AIC delay times reflect the evolutionary timescale of the donor. In particular, if we allow a WD to accrete via a wind from an evolved (AGB) star, the AIC birthrates are noticeably enhanced, and can easily occur with delay times < 100 Myr.

We find that our AIC and MIC rates, calculated with the STARTRACK code, are in agreement with those found by Hurley et al. (2010) (BSE code) and Lyutikov & Toonen (2017) (SeBa code), respectively. Our present work substantiates the need to consider NSs formed via induced collapse as an important channel for NS formation. In the future, when WD binaries can be resolved through gravitational radiation (e.g. LISA for Galactic binaries, and DECIGO and BBO which will be sensitive to extra-Galactic binaries, too), measuring their chirp masses will be possible, and will

be useful in constraining the evolutionary origin of these sources. As we have shown, it may be possible to set limits on CE physics by determining chirp masses of double WDs, since the two CE prescriptions adopted here exhibit distinct M_{chirp} distribution shapes (Figs. 7 and 8). With the exception of the most massive, shortest orbital period double WD systems prior to merger (see Fig. 9), most MIC NSs in M31 will probably be too far to measure their gravitational wave strain amplitude at time of merger, though such systems within our own Galaxy and other nearby galaxies (LMC, SMC) have a very good chance at being detected with future space-based gravitational wave observatories. The main challenge in observing an electromagnetic counterpart for such a gravitational wave event is the low MIC birthrate itself, which we estimate to be only a few $\times 10^{-4}$ per year in the Galaxy today; roughly an order of magnitude below the observationally-inferred Galactic SN Ia rate.

We remind the reader that our simulations assume field evolution only, e.g. no N-body interactions. On the other hand, N-body interactions are only important in dense environments, such as globular clusters, thus the rate estimates presented in this work are most relevant for the Galactic disk. Among higher stellar densities, stellar exchange interactions are likely to occur, which alters the evolutionary outcome of the stars. These additional interactions would likely lead to a higher number of AIC and MIC progenitor systems being created, which may be an important link toward understanding the formation of double NS mergers such as GW170817 (see [Belczynski et al. 2017](#), figure 2).

ACKNOWLEDGEMENTS

Excellence for All-sky Astrophysics (CAASTRO) through project number CE110001020, and grant FT170100243. KB acknowledges support from the Polish National Science Center (NCN) grant: Sonata Bis 2 DEC-2012/07/E/ST9/01360. IRS acknowledges funding from the Australian Research Council under grant FT160100028. AJR thanks Stuart Sim for helpful comments and Bernhard Müller, Jarrod Hurley, Tyrone Woods, and Christopher Berry for discussion. Parts of this work made use of WebPlotDigitizer version 4 <https://automeris.io/WebPlotDigitizer>.

6 APPENDIX

In this section we describe the evolutionary pathway leading to the formation of MIC and AIC progenitors in more detail. We focus on 4 specific examples.

Example 1: Classical CE model, AIC, medium-long delay time: The following evolutionary example showcases the evolution of an AIC system that evolves into a NS+HeWD binary, though with an orbital period that is larger than those typical for redbacks (see Discussion). The ZAMS masses are 7.2 and $1.4 M_{\odot}$ with a separation of $2310 R_{\odot}$. The first interaction occurs at 53 Myr after starburst when there is a CE phase between the late AGB primary ($5.8 M_{\odot}$) and the main sequence ($1.4 M_{\odot}$) companion. The CE phase causes the orbit to decrease from $1923 R_{\odot}$ to $31 R_{\odot}$ and the AGB core evolves into a ONe WD. The next interaction doesn't occur until 3409 Myr after starburst when there is

stable Roche-lobe overflow between the red giant ($1.4 M_{\odot}$) secondary and the ONe WD ($1.3 M_{\odot}$). Mass transfer lasts a few Myr, initially proceeding on a thermal timescale, until AIC occurs at 3411 Myr resulting in a NS ($1.26 M_{\odot}$) and the red giant is left with a mass of $0.96 M_{\odot}$ (with a core mass of $0.25 M_{\odot}$) with an orbital separation of $38 R_{\odot}$ (18 days). A few Myr later, mass transfer is re-initiated when the red giant fills its Roche-lobe again. Mass transfer ceases when the stars have attained an orbital separation of $150 R_{\odot}$ (156 days) and the masses are $1.5 M_{\odot}$ (NS) and $0.35 M_{\odot}$ (red giant; core mass $0.32 M_{\odot}$). The secondary shortly thereafter evolves into a helium WD ($0.34 M_{\odot}$). The system is found at a Hubble time with component masses $1.5 M_{\odot}$ (NS), $0.34 M_{\odot}$ (He WD) with an orbital separation of $160 R_{\odot}$.

Example 2: Classical CE model, MIC, very long delay time: We describe an example of a system that attains very high gravitational wave frequencies (orbital periods ~ 10 s of seconds, or $f_{\text{gw}} > 0.08$, compare Figs 9 and 10) at time of the WD-WD merger. Such MIC systems, with final WD masses $\gtrsim 1.2 M_{\odot}$ each, do not appear in the new CE model. The chirp mass of this system falls near the second peak in Fig. 7, at $M_{\text{chirp}} = 1.06$. The ZAMS masses are 8.5 and $7.0 M_{\odot}$ with a separation of $62 R_{\odot}$. Stable Roche-lobe overflow starts between the Hertzsprung Gap primary and the MS companion at 33 Myr post-starburst. RLOF continues until the orbital separation reaches $340 R_{\odot}$ at which time mass transfer ceases. By this time, the evolved primary is $1.7 M_{\odot}$ and the secondary has attained a mass of $10.3 M_{\odot}$. At 40 Myr, mass transfer is re-established between the H-envelope stripped (via previous mass transfer), helium-burning subgiant which fills its Roche-lobe and the MS secondary, and RLOF continues for a short time (< 1 Myr) until an orbital separation of $640 R_{\odot}$. The primary shortly thereafter evolves into a CO WD. At 46 Myr the secondary starts to evolve up the red giant branch, and at an orbital separation of $442 R_{\odot}$ there is a CE between the red giant secondary and the CO WD. The system then consists of stars with masses $1.2 M_{\odot}$ (CO WD), $2.3 M_{\odot}$ (H-envelope stripped, He-burning star), and an orbital period of $3.9 R_{\odot}$. The secondary shortly thereafter becomes an evolved H-stripped, He-burning star and initiates RLOF toward the CO WD primary at 50 Myr. Mass transfer steadily continues until the secondary evolves into a ONe WD. The MIC progenitor is found with an orbital separation of $3.9 R_{\odot}$ and component masses 1.2 and $1.2 M_{\odot}$ for the CO and ONe WD. The system loses orbital angular momentum due to gravitational wave emission and the stars merge at 10097 Myr. We note that this system falls above the maximum threshold assumed for NS masses in [Margalit & Metzger \(2017\)](#), making it a viable stellar mass black hole candidate.

Example 3: New CE model, MIC, short delay time: This system appears in the chirp mass distribution peak (see Fig. 8). In this short delay time channel example, the ZAMS masses are 7.4 and $5.2 M_{\odot}$ with a separation of $818 R_{\odot}$. The initial primary fills its Roche lobe while in the Hertzsprung Gap and the main sequence secondary accretes matter stably, even after the primary evolves up the Red Giant Branch. After the orbit has become very wide (445 d) mass transfer ceases, and soon after the primary becomes a H-envelope-stripped, helium-burning star. The secondary, now more massive than its ZAMS mass, becomes a Red Giant and when it fills its Roche lobe, mass transfer is unstable, and a

CE phase follows. Upon emerging from the CE, the system consists of a double helium-burning star binary where both stars have lost their envelopes, e.g. a double sdB star (see [Kupfer et al. 2015](#), for observed examples of similar, lower-mass analogue systems), with an orbital period of 6.6 days and stellar masses of 1.27 and 1.91 M_{\odot} , respectively. Shortly thereafter the primary evolves into a (helium) giant, and transfers mass stably to the (still compact) helium-burning star companion. After the primary evolves into a CO WD, and the secondary becomes a (helium) giant, the system soon encounters a second CE phase where, yet again, the secondary star loses its envelope (this time its helium-rich envelope). Upon emerging from the CE, the binary consists of a CO WD and an ONe WD (masses 0.85 and 1.21 M_{\odot} , respectively) with an orbital period of 24 minutes.

Example 4: New CE model, AIC, short delay time: This example showcases a common channel in which the NS is formed via stable Roche-lobe overflow accretion on a ONe WD from the wind of an evolved AGB star. The stars start out on the ZAMS with masses 7.6 and 5.6 M_{\odot} with an orbital separation of 6150 R_{\odot} . The primary evolves into a ONe WD at 47 Myr; by this time the orbit has increased in size to 10652 R_{\odot} (stellar masses are 1.37 and 6.63 M_{\odot}). At 81 Myr post-starburst, the secondary becomes an evolved (thermally-pulsating) AGB star (6.4 M_{\odot} ; core mass 1.2 M_{\odot}), and at this stage the ONe WD companion begins to accrete some mass lost in the AGB wind. By 82 Myr, the primary turns into a NS via AIC. The NS continues to accrete via the AGB wind, until the AGB star evolves into a CO WD (within 0.1 Myr). The final component masses are 1.28 and 1.23 M_{\odot} for the NS and CO WD, respectively, on an orbit with separation of 24 days.

References

- Abate C., Pols O. R., Izzard R. G., Mohamed S. S., de Mink S. E., 2013, *A&A*, 552, A26
- Atlee D. W., Assef R. J., Kochanek C. S., 2009, *ApJ*, 694, 1539
- Backus P. R., Taylor J. H., Damashek M., 1982, *ApJL*, 255, L63
- Badenes C., Maoz D., 2012, *ApJL*, 749, L11
- Bailyn C. D., Grindlay J. E., 1990, *ApJ*, 353, 159
- Belczynski K. et al., 2017, *ArXiv e-prints*
- Belczynski K., Bulik T., Fryer C. L., Ruiter A., Valsecchi F., Vink J. S., Hurley J. R., 2010a, *ApJ*, 714, 1217
- Belczynski K., Holz D. E., Bulik T., O’Shaughnessy R., 2016, *Nature*, 534, 512
- Belczynski K., Kalogera V., Bulik T., 2002, *ApJ*, 572, 407
- Belczynski K., Kalogera V., Rasio F. A., Taam R. E., Zezas A., Bulik T., Maccarone T. J., Ivanova N., 2008, *ApJS*, 174, 223
- Belczynski K., Lorimer D. R., Ridley J. P., Curran S. J., 2010b, *MNRAS*, 407, 1245
- Belczynski K., Taam R. E., 2004, *ApJ*, 603, 690
- Belczynski K., Taam R. E., Kalogera V., Rasio F. A., Bulik T., 2007, *ApJ*, 662, 504
- Benacquista M. J., Portegies Zwart S., Rasio F. A., 2001, *Classical and Quantum Gravity*, 18, 4025
- Bensby T. et al., 2013, *A&A*, 549, A147
- Bildsten L., Shen K. J., Weinberg N. N., Nelemans G., 2007, *ApJL*, 662, L95
- Boyles J., Lorimer D. R., Turk P. J., Mnatsakanov R., Lynch R. S., Ransom S. M., Freire P. C., Belczynski K., 2011, *ApJ*, 742, 51
- Brooks J., Schwab J., Bildsten L., Quataert E., Paxton B., 2017, *ApJ*, 843, 151
- Brown W. R., Kilic M., Kosakowski A., Gianninas A., 2017, *ApJ*, 847, 10
- Buell J. F., 2013, *MNRAS*, 428, 2577
- Cescutti G., Chiappini C., 2014, *A&A*, 565, A51
- Chantereau W., Charbonnel C., Decressin T., 2015, *A&A*, 578, A117
- Chruslinska M., Belczynski K., Klencki J., Benacquista M., 2018, *MNRAS*, 474, 2937
- Chung C., Yoon S.-J., Lee Y.-W., 2011, *ApJ*, 740, L45
- Cornish N., Robson T., 2017, in *Journal of Physics Conference Series*, Vol. 840, *Journal of Physics Conference Series*, p. 012024
- Côté B., Denissenkov P., Herwig F., Ruiter A. J., Ritter C., Pignatari M., Belczynski K., 2017a, *ArXiv e-prints*
- Côté B. et al., 2017b, *ArXiv e-prints*
- Crocker R. M. et al., 2017, *Nature Astronomy*, 1, 0135
- Dan M., Guillochon J., Brüggem M., Ramirez-Ruiz E., Rosswog S., 2015, *MNRAS*, 454, 4411
- Darbha S., Metzger B. D., Quataert E., Kasen D., Nugent P., Thomas R., 2010, *MNRAS*, 1254
- de Kool M., 1990, *ApJ*, 358, 189
- De Marco O., 2009, *PASP*, 121, 316
- De Marco O., Passy J.-C., Moe M., Herwig F., Mac Low M.-M., Paxton B., 2011, *MNRAS*, 411, 2277
- De Silva G. M. et al., 2015, *MNRAS*, 449, 2604
- Dessart L., Burrows A., Ott C. D., Livne E., Yoon S.-C., Langer N., 2006, *ApJ*, 644, 1063
- Dominik M., Belczynski K., Fryer C., Holz D. E., Berti E., Bulik T., Mandel I., O’Shaughnessy R., 2012, *ApJ*, 759, 52
- Fenn D., Plewa T., Gawryszczak A., 2016, *MNRAS*, 462, 2486
- Ferrario L., Wickramasinghe D., 2007, *MNRAS*, 375, 1009
- Freire P. C. C., 2013, in *IAU Symposium*, Vol. 291, *Neutron Stars and Pulsars: Challenges and Opportunities after 80 years*, van Leeuwen J., ed., pp. 243–250
- Freire P. C. C., Tauris T. M., 2014, *MNRAS*, 438, L86
- Fryer C., Benz W., Herant M., Colgate S. A., 1999, *ApJ*, 516, 892
- Fryer C. L., Belczynski K., Wiktorowicz G., Dominik M., Kalogera V., Holz D. E., 2012, *ApJ*, 749, 91
- Fryer C. L., Kusenko A., 2006, *ApJS*, 163, 335
- Gratton R. G., Carretta E., Bragaglia A., 2012, *A&A Rev.*, 20, 50
- Grindlay J. E., 1987, in *IAU Symposium*, Vol. 125, *The Origin and Evolution of Neutron Stars*, Helfand D. J., Huang J.-H., eds., pp. 173–184
- Hamann W.-R., Koesterke L., 1998, *A&A*, 335, 1003
- Hillebrandt W., Nomoto K., Wolff R. G., 1984, *A&A*, 133, 175
- Hurley J. R., Tout C. A., Pols O. R., 2002, *MNRAS*, 329, 897
- Hurley J. R., Tout C. A., Wickramasinghe D. T., Ferrario L., Kiel P. D., 2010, *MNRAS*, 402, 1437
- Ivanova N., Chaichenets S., 2011, *ApJL*, 731, L36

- Ivanova N., Heinke C. O., Rasio F. A., Belczynski K., Fregeau J. M., 2008, *MNRAS*, 386, 553
- Ivanova N. et al., 2013, *A&A Rev.*, 21, 59
- Ivanova N., Taam R. E., 2004, *ApJ*, 601, 1058
- Janka H.-T., 2017, *ApJ*, 837, 84
- Jones S. et al., 2013, *ApJ*, 772, 150
- Jones S., Röpke F. K., Pakmor R., Seitzzahl I. R., Ohlmann S. T., Edelmann P. V. F., 2016, *A&A*, 593, A72
- Karakas A. I., 2014, *MNRAS*, 445, 347
- Karakas A. I., Marino A. F., Nataf D. M., 2014, *ApJ*, 784, 32
- Katz J. I., 1975, *Nature*, 253, 698
- Kremer K., Breivik K., Larson S. L., Kalogera V., 2017, *ApJ*, 846, 95
- Kromer M. et al., 2015, *MNRAS*, 450, 3045
- Kroupa P., Tout C. A., Gilmore G., 1993, *MNRAS*, 262, 545
- Kupfer T. et al., 2015, *A&A*, 576, A44
- Kwiatkowski D., 2015, *ArXiv e-prints*
- Lipunov V. M., 2017, *New Astronomy*, 56, 84
- Livio M., Soker N., 1988, *ApJ*, 329, 764
- Lyne A. G., Manchester R. N., D'Amico N., 1996, *ApJL*, 460, L41
- Lyutikov M., Toonen S., 2017, *ArXiv e-prints*
- Manchester R. N., Hobbs G. B., Teoh A., Hobbs M., 2005, *VizieR Online Data Catalog*, 7245
- Maoz D., Hallakoun N., Badenes C., 2018, *ArXiv e-prints*
- Maoz D., Mannucci F., Nelemans G., 2014, *ARA&A*, 52, 107
- Margalit B., Metzger B. D., 2017, *ApJL*, 850, L19
- Marquardt K. S., Sim S. A., Ruiter A. J., Seitzzahl I. R., Ohlmann S. T., Kromer M., Pakmor R., Röpke F. K., 2015, *A&A*, 580, A118
- Metzger B. D., Piro A. L., Quataert E., 2009, *MNRAS*, 396, 1659
- Miyaji S., Nomoto K., Yokoi K., Sugimoto D., 1980, *PASJ*, 32, 303
- Moe M., Di Stefano R., 2017, *ApJS*, 230, 15
- Mohamed S., Podsiadlowski P., 2007, in *Astronomical Society of the Pacific Conference Series*, Vol. 372, 15th European Workshop on White Dwarfs, Napiwotzki R., Burleigh M. R., eds., p. 397
- Moore K., Townsley D. M., Bildsten L., 2013, *ApJ*, 776, 97
- Moriya T. J., 2016, *ApJL*, 830, L38
- Nataf D. M., Gould A. P., 2012, *ApJL*, 751, L39
- Nataf D. M., Udalski A., Gould A., Pinsonneault M. H., 2011, *ApJ*, 730, 118
- Nelemans G., 2005, in *Astronomical Society of the Pacific Conference Series*, Vol. 330, *The Astrophysics of Cataclysmic Variables and Related Objects*, J.-M. Hameury & J.-P. Lasota, ed., pp. 27–40
- Nelemans G., 2013, in *Astronomical Society of the Pacific Conference Series*, Vol. 467, 9th LISA Symposium, Auger G., Binétruy P., Plagnol E., eds., p. 27
- Nelemans G., Yungelson L. R., Portegies Zwart S. F., 2004, *MNRAS*, 349, 181
- Nomoto K., 1987, *ApJ*, 322, 206
- Nomoto K., Iben, Jr. I., 1985, *ApJ*, 297, 531
- Nomoto K., Kondo Y., 1991, *ApJL*, 367, L19
- Ohlmann S. T., Röpke F. K., Pakmor R., Springel V., 2016, *ApJL*, 816, L9
- Pakmor R., Kromer M., Röpke F. K., Sim S. A., Ruiter A. J., Hillebrandt W., 2010, *Nature*, 463, 61
- Pakmor R., Kromer M., Taubenberger S., Sim S. A., Röpke F. K., Hillebrandt W., 2012, *ApJL*, 747, L10
- Pakmor R., Kromer M., Taubenberger S., Springel V., 2013, *ApJL*, 770, L8
- Pavlovskii K., Ivanova N., 2015, *MNRAS*, 449, 4415
- Perets H. B. et al., 2010, *Nature*, 465, 322
- Piro A. L., Kollmeier J. A., 2016, *ApJ*, 826, 97
- Podsiadlowski P., Langer N., Poelarends A. J. T., Rappaport S., Heger A., Pfahl E., 2004, *ApJ*, 612, 1044
- Ricker P. M., Taam R. E., 2012, *ApJ*, 746, 74
- Röpke F. K., Hillebrandt W., Schmidt W., Niemeyer J. C., Blinnikov S. I., Mazzali P. A., 2007, *ApJ*, 668, 1132
- Rosenfield P. et al., 2012, *ApJ*, 755, 131
- Ruiter A. J., Belczynski K., Benacquista M., Larson S. L., Williams G., 2010, *ApJ*, 717, 1006
- Ruiter A. J., Belczynski K., Fryer C., 2009, *ApJ*, 699, 2026
- Ruiter A. J., Belczynski K., Sim S. A., Seitzzahl I. R., Kwiatkowski D., 2014, *MNRAS*, 440, L101
- Ruiter A. J. et al., 2013, *MNRAS*, 429, 1425
- Saio H., Nomoto K., 1985, *A&A*, 150, L21
- Salaris M., Cassisi S., 2005, *Evolution of Stars and Stellar Populations*. p. 400
- Schwab J., Quataert E., Kasen D., 2016, *MNRAS*, 463, 3461
- Seitzzahl I. R. et al., 2013, *MNRAS*, 429, 1156
- Shen K. J., Moore K., 2014, *ApJ*, 797, 46
- Shingles L. J., Doherty C. L., Karakas A. I., Stancliffe R. J., Lattanzio J. C., Lugaro M., 2015, *MNRAS*, 452, 2804
- Siess L., 2006, *A&A*, 448, 717
- Smedley S. L., Tout C. A., Ferrario L., Wickramasinghe D. T., 2015, *MNRAS*, 446, 2540
- Smedley S. L., Tout C. A., Ferrario L., Wickramasinghe D. T., 2017, *MNRAS*, 464, 237
- Smith N., 2014, *ARA&A*, 52, 487
- Sweigart A. V., 1987, *ApJS*, 65, 95
- Tanikawa A., Nakasato N., Sato Y., Nomoto K., Maeda K., Hachisu I., 2015, *ApJ*, 807, 40
- Tauris T. M., Sanyal D., Yoon S.-C., Langer N., 2013, *A&A*, 558, A39
- Timmes F. X., Woosley S. E., Weaver T. A., 1996, *ApJ*, 457, 834
- Toonen S., Claeys J. S. W., Mennekens N., Ruiter A. J., 2014, *A&A*, 562, A14
- van den Heuvel E. P. J., Bonsema P. T. J., 1984, *A&A*, 139, L16
- van Kerkwijk M. H., Chang P., Justham S., 2010, *ApJL*, 722, L157
- Vennes S., Nemeth P., Kawka A., Thorstensen J. R., Khalack V., Ferrario L., Alper E. H., 2017, *Science*, 357, 680
- Vink J. S., de Koter A., 2005, *A&A*, 442, 587
- Wanajo S., Janka H.-T., Müller B., 2011, *ApJL*, 726, L15
- Webbink R. F., 1984, *ApJ*, 277, 355
- Wiktorowicz G., Belczynski K., Maccarone T., 2014, in *Binary Systems, their Evolution and Environments*, p. 37
- Woods T. E., Ghavamian P., Badenes C., Gilfanov M., 2017, *Nature Astronomy*, 1, 800
- Woosley S. E., Heger A., 2015, *ApJ*, 810, 34
- Wu C., Wang B., 2017, *ArXiv e-prints*
- Xu X.-J., Li X.-D., 2010a, *ApJ*, 722, 1985
- Xu X.-J., Li X.-D., 2010b, *ApJ*, 716, 114

- Yagi K., Seto N., 2017, Phys. Rev. D, 95, 109901
Yoon S., Langer N., 2005, A&A, 435, 967
Yungelson L., Livio M., 1998, ApJ, 497, 168
Zapartas E. et al., 2017, A&A, 601, A29